1 Quarkonia

Coordinators: Anton Andronic (Münster University) and Emilien Chapon (CERN)

Contributors: E. Ferreiro (Santiago de Compostela University), J.-P. Lansberg (Institut the Physique Nucléaire d'Orsay), R. Rapp (Texas A&M University), J. Castillo Castellanos (CEA Saclay), C. Cheshkov (IPN Lyon), J. Martin Blanco (Laboratoire Leprince Ringuet), J. Park (Korea University), X. Du (Texas A&M University), M. Strickland (Kent State University), R. Venugopalan (BNL), I. Vitev (Los Alamos National Laboratory)

1.1 Introduction

A key objective in high-energy heavy-ion physics is to determine the in-medium forces that give rise to the remarkable many-body features of the QGP. In the QCD vacuum, the unravelling of the fundamental force between two static Color charges was made possible by the discovery of the charmonium and bottomonium states in the 1970's. Subsequent quantitative analyses of the bound-state spectra established a phenomenological potential of the Cornell type [1],

$$V(r) = -\frac{4}{3}\frac{\alpha_s}{r} + \sigma r \ , \tag{1}$$

with a colour-Coulomb term due to gluon exchange dominant at short distances, and a linear term with string tension $\sigma \simeq 0.9\,\mathrm{GeV/fm}$ to account for confinement at large distance. This potential has also been quantitatively confirmed by lattice-QCD (lQCD) calculations [2, 3]. The corresponding effective field theory of QCD, potential non-relativistic QCD (pNRQCD), allows for the definition of the static potential [4] in a $1/m_Q$ expansion for large heavy-quark mass, m_Q [5,6]. The heavy-quark (HQ) potential thus provides a well calibrated starting point to probe the QCD medium, and the in-medium spectroscopy of quarkonia is the natural tool to carry this out in heavy-ion collisions, cf. [7–11] for recent reviews. The string term in the HQ potential, eq. (1), characterises the long-range nonperturbative part of the force and is associated with the confining property of QCD. It is expected to play a critical role in the transition from hadronic to partonic degrees of freedom, and may be responsible for the remarkable transport properties of the QGP, *i.e.*, its strongly coupled nature, up to temperatures of 2-3 times the (pseudo-)critical temperature, T_{c} [12].

Much like in vacuum, a systematic investigation of the in-medium force must involve the *spectroscopy* of different states, as they subsequently dissolve with increasing temperature. The complexity in describing the in-medium properties of quarkonia and their implementation into transport calculations in heavy-ion collisions prevents their use as a straightforward thermometer of the medium produced in these reactions. On the contrary, using information on the space-time and temperature evolution in heavy-ion collisions from other sources (e.g.,, hydrodynamics and electromagnetic radiation), on can utilize quarkonium observables to deduce their in-medium properties and infer the fundamental interactions in QCD matter. In the vacuum, only the 1S ground-state bottomonia ($\Upsilon(1\mathrm{S})$ and η_{b}) are small enough in size to be mostly bound by the colour-Coulomb force. All excited bottomonia and all charmonia are predominantly bound by the nonperturbative string term (and/or residual mesonic forces). Thus, charmonia and excited bottomonia are excellent probes of the in-medium confining force, as originally envisioned for the J/ψ [13]. However, in the cooling of the expanding fireball, quarkonia can also be "(re)generated" through recombination of individual heavy quarks and anti-quarks diffusing through the medium. It is important to emphasise that quarkonium formation occurs also from quarks and antiquarks from different initial pairs. This mechanism [14–16] has turned out to be critical in understanding the rise of J/ψ production from RHIC to the LHC where (re)generation seems to constitute the major part of the yield observed in central Pb–Pb collisions [17]. The data is also compatible with production of J/ψ exclusively through statistical hadronisation at the crossover phase boundary [18]. Precise measurements of the $c\bar{c}$ production cross section and the extraction of the charm-quark diffusion coefficient in Runs 3 & 4 will be important for making a more definite statement; these are key objectives discussed in the chapter **??** on open heavy-flavor production. Information from p_{T} spectra and elliptic flow will help to complete the picture.

Regarding bottomonia, the current understanding suggests that (re)generation is less important for $\Upsilon(1S)$, but possibly figures as a major component in the strongly suppressed yield of excited states [19, 20]. It is therefore of great importance to obtain additional information about the typical time at which quarkonia are produced, in particular through p_T spectra and elliptic flow which contain information about the fireball collectivity imprinted on the quarkonia by the time of their decoupling. A schematic illustration of the current knowledge extracted from in-medium quarkonium spectroscopy, *i.e.*, their production systematics in heavy-ion collisions is shown in Fig. 1.

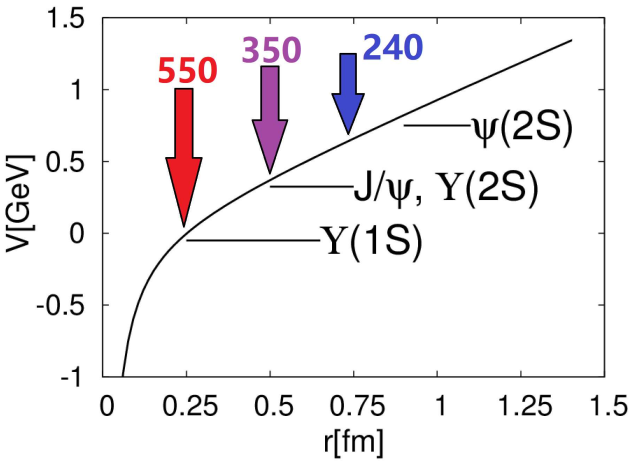

Fig. 1: The vacuum heavy-quark potential as a function of $Q\bar{Q}$ separation. The horizontal lines indicate the approximate locations of the vacuum bound states while the vertical arrows indicate the minimal screening distances of the media produced at the SPS, RHIC and LHC, as deduced from approximate initial temperatures reached in these collisions extracted from data (indicated above the arrows in MeV) and from quarkonium production systematics in Pb–Pb and Au-Au collisions. Figure taken from Ref. [17].

On the theoretical side, the basic objects are the quarkonium spectral functions which encode the information on the quarkonium binding energies, in-medium HQ masses and the (inelastic) reaction rates. Ample constraints on the determination of the quarkonium spectral functions are available from thermal lQCD, *e.g.*, in terms of the heavy-quark free energy, euclidean and spatial quarkonium correlation functions, and HQ susceptibilities, and are being implemented into potential model calculations [21–27]. In particular, the role of dissociation reactions has received increasing attention. Early calculations of gluo-dissociation [28, 29] or inelastic parton scattering [30] have been revisited and reformulated, e.g., as a singlet-to-octet transition mechanism [24] or in terms of an imaginary part of a two-body potential [31], respectively. In particular, the latter accounts for interference effects which reduce the rate relative to “quasi-free” dissociation [30] in the limit of small binding; interference effects can also be calculated diagrammatically [32]; they ensure that, in the limit of vanishing size, a Color-neutral $Q\bar{Q}$ dipole becomes “invisible” to the Color charges in the QGP.

The information from the spectral functions can then be utilised in heavy-ion phenomenology via transport models. The latter provide the connection between first-principles information from lQCD and experiment that greatly benefits the extraction of robust information on the in-medium QCD force and its emergent transport properties, most notably the (chemical) equilibration rates of quarkonia. Thus far most transport models are based on rate equations and/or semiclassical Boltzmann equations. In recent years quantum transport approaches have been developed using, e.g., a Schrödinger-Langevin [33–36] or density-matrix [37, 38] formulation. These will enable to test the classical approximation underlying the Boltzmann and rate equation treatments and ultimately quantify the corrections. Quantum effects may be particularly relevant at high p_{T} in connection with the in-medium formation times of quarkonia, augmented by the Lorentz time dilation in the moving frame; schematic treatments of this effect in semiclassical approaches suggest that varying formation times can leave observable differences for high-momentum charmonia and bottomonia [19, 20, 39–41]. Finally, the implementation of phase-space distributions of explicitly diffusing heavy quarks into quarkonium transport is being investigated by various groups (see, e.g., Ref. [42]), which, as mentioned above, will provide valuable constraints on the magnitude and p_{T} dependence of (re)generation processes. In particular, the role of non-perturbative effects in the HQ interactions in the QGP (which are believed to be essential to explain the large elliptic flow observed for D-mesons [43]) needs to be accounted for; the associated large scattering widths are likely to require quarkonium transport implementations beyond semi-classical (or perturbative) approximations, which reiterates the need for a quantum treatment of recombination processes.

The larger experimental data samples in Runs 3 & 4, combined with improved detector performance and measurement techniques, will allow one to significantly improve over the current measurements, with extended kinematic coverage (in p_{T}) and allowing one to reach also currently-unobserved quarkonium states, like $\Upsilon(3\mathrm{S})$. The complementarity (and overlap) of all 4 LHC experiments is crucial in this endeavour and will call for a data combination strategy, for instance for Υ azimuthal anisotropy. Quarkonia are measured in the dimuon channel in ATLAS ($|y| < 2.0$), CMS ($|y| < 2.4$), LHCb ($2.0 < y < 4.5$), and ALICE ($2.5 < y < 4.0$), and in the dielectron channel with ALICE ($|y| < 0.9$). We present below data projections and simulations for a selection of observables and compare to model predictions (which sometimes constitute the basis for the projections). The model uncertainties shown in this section represent the current knowledge; significant improvements are expected both in what concerns the conceptual aspects discussed above as well for the input parameters, which will be constrained by data and theory (for instance in what concerns nuclear PDFs, see also Section **??**).

All four LHC experiments will benefit from a large upgrade program, during the Long Shutdown 2 (2019–2020) for ALICE and LHCb, and during Long Shutdown 3 (2024–2025) for ATLAS and CMS. The addition of the Muon Forward Tracker (MFT) will allow ALICE to separate the prompt charmonium from the contribution from B meson decays. In addition, the background will be reduced, yielding to better signal over background ratios. Regarding ATLAS and CMS, the upgraded inner tracker will extend to $|\eta| \lesssim 4.0$ after LS3, and the muon system coverage to $|\eta| \lesssim 2.7$ (3.0) for ATLAS (CMS). While the detector improvements will have a smaller impact than the increase in data sample size, this increase in pseudorapidity coverage is appreciable in also giving an overlap with the range of ALICE and LHCb. Better track momentum resolution is also expected from these upgraded inner trackers, with an improvement of about 30% of the mass resolution of quarkonia for CMS [44]. The expected improvement in the relative statistical uncertainty, due to a better signal over background ratio, is in the range 10–25% [45].

1.2 Charmonia in Pb–Pb collisions

A remarkable discovery at the LHC was that the suppression of J/ψ is significantly reduced in comparison to lower energies [46] and that this reduction is concentrated at lower p_{T} [47, 48], compatible with predictions of (re)generation at the phase boundary of QCD [14] or throughout the deconfined phase [15, 49, 50], via recombination of diagonal (correlated pairs) or off-diagonal $\mathrm{c\bar{c}}$ pairs [16]. No significant difference is however found between measurements at $\sqrt{s_{\mathrm{NN}}} = 2.76\,\mathrm{TeV}$ and $\sqrt{s_{\mathrm{NN}}} = 5.02\,\mathrm{TeV}$ [48, 51]. Recently, the measurement of a significant elliptic flow coefficient v_2 both for D mesons [52–54] and J/ψ [55–59], which was shown to be correlated to the flow of the bulk particles [59, 60], can be seen as another indication for the thermalisation of charm quarks in the QGP. Transport model calculations [61, 62] currently underestimate the data for $p_{\mathrm{T}} \gtrsim 6$ GeV/c [55, 57, 58].

The projected ALICE measurement of inclusive J/ψ v_2 as a function of p_{T} for the centrality class 20–40%, for $2.5 < y < 4$, in comparison to model calculations [62] is shown in Fig. 2. Disentangling the contributions of prompt and non-prompt J/ψ and considering (path-length dependent) energy loss

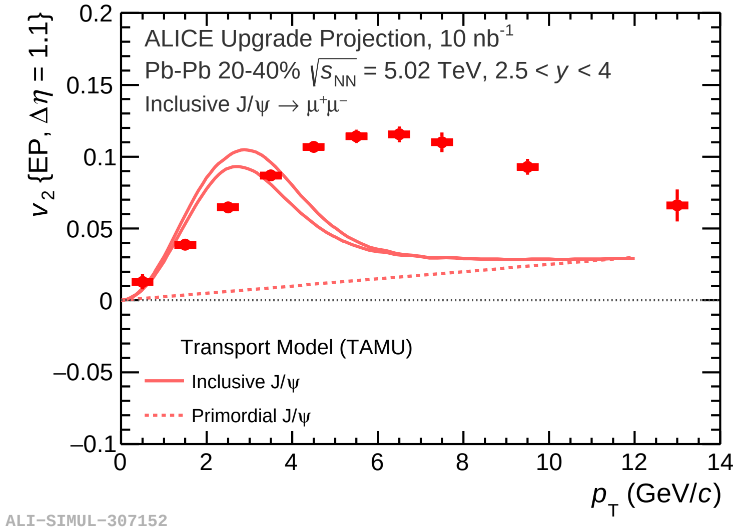

Fig. 2: Projected measurement of elliptic flow coefficient v_2 as a function of p_T for J/ψ mesons (measured in ALICE, for $2.5 < y < 4$), for the centrality class 20–40%, in comparison to model calculations [62].

seems mandatory to understand the details of the J/ψ v_2 pattern, which will be facilitated with the detector upgrades and higher luminosity of Runs 3 & 4. The measurement of higher harmonics, e.g., v_3, which are sensitive to initial state energy density fluctuations, will also become available and provide further insight into the charmonium production mechanisms. Precise prompt and non-prompt J/ψ v_2 and v_3 measurements at low p_T will be reachable using the ALICE central barrel. Polarisation will be measured too [63], providing further insight in the different production mechanisms involved in Pb–Pb collisions as compared to pp. Under the statistical hadronisation paradigm, the prompt J/ψ yield in Pb–Pb collisions should be unpolarised with the 3 polarisation states equally populated.

At high p_T, where a raising trend is currently hinted by Run 2 R_{AA} measurements [51, 64], the production mechanisms cannot currently be resolved, given the statistical limitation in the data (see Fig. 3, left). The high p_T reach of Runs 3 & 4 data (illustrated in Fig. 3 (right) for CMS) will allow one to conclude on the important question of whether J/ψ formation at high p_T is determined by the Debye screening mechanism [41, 65], or by energy loss of the charm quark or the $c\bar{c}$ pair [66, 67].

The measurement of ψ(2S) mesons is more difficult than that of J/ψ, because of a much smaller production cross section times branching ratio and even larger suppression in Pb–Pb, yielding a very low signal to background ratio. The projections for the measurement of the ψ(2S) state in ALICE are shown in Fig. 4 as a function of centrality and compared to model predictions in the transport approach [62] and from the statistical hadronisation model [18]. This (p_T-integrated) measurement will significantly contribute to make a distinction between the two models. Projections are also available from the CMS experiment [69]. Other states, for instance χ_c, may be measured too, albeit the measurement down to $p_T = 0$ will remain challenging. B_c^+ mesons can also be measured, either in the J/$\psi\pi$ or J/$\psi\mu\nu_\mu$ channel, to further study recombination in the beauty sector.

1.3 Bottomonia in Pb–Pb collisions

The study of bottomonia with Pb–Pb data from the Runs 3 & 4 of the LHC will bring further information on the physics aspects described above. Although their production is a priori sensitive to the same effects as charmonia, in practice the two quarkonium families feature some fundamental differences. Binding

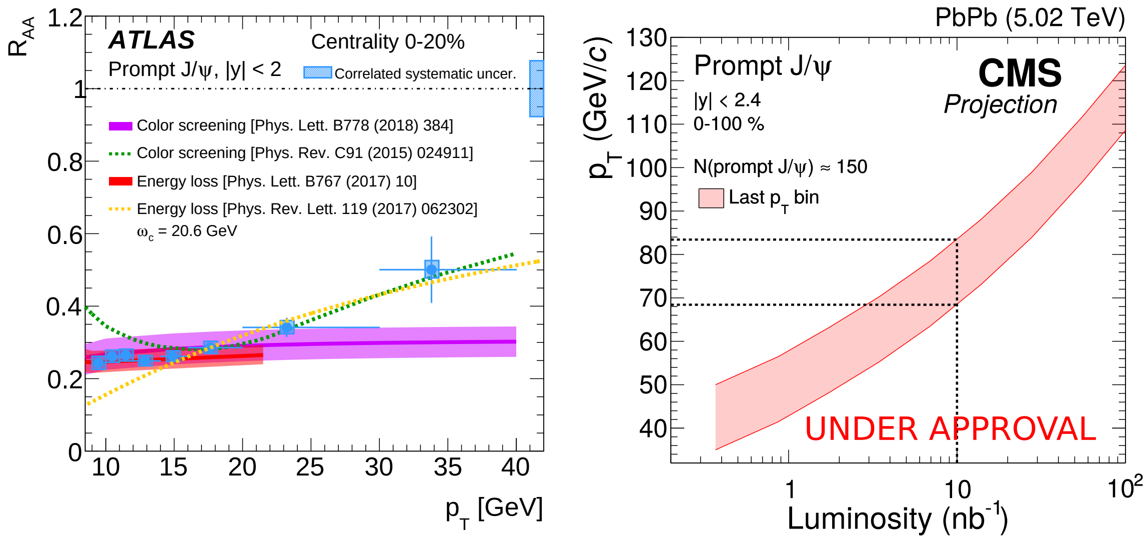

Fig. 3: Left: R_{AA} vs p_{T} for prompt J/ψ in central (0–20%) collisions (ATLAS, $|y| < 2$, [64]). Right: Prompt J/ψ high p_{T} bin boundaries as a function of luminosity with the CMS experiment [45]. The boundaries are chosen in such a way the number of mesons in the bin for the corresponding luminosity equals the number of mesons found in the last p_{T} bin of the current measurement [51].

energies differ, which is reflected in the different dissociation temperatures. Experimentally, compared to charmonia, the absence of contribution from B meson decays and the more similar cross section times branching ratio between the ground and excited states make bottomonia measurements easier. At the same time, in pp collisions, up to 30–50% of the measured $\Upsilon(1\mathrm{S})$ and $\Upsilon(2\mathrm{S})$ yields actually result from the feed-down from other states [70, 71]: a large portion of measured $\Upsilon(1\mathrm{S})$ suppression can be due to the stronger suppression of the feed-down states – $\Upsilon(2\mathrm{S})$ and $\Upsilon(3\mathrm{S})$ mesons also receive a significant contribution from feed-down. The impact of (re)generation from uncorrelated $\mathrm{b\bar{b}}$ is also expected to be much smaller than for charmonia, because of the much smaller number of $\mathrm{b\bar{b}}$ pairs per Pb–Pb event compared to that of $\mathrm{c\bar{c}}$ pairs. The importance of regeneration for bottomonia, from correlated or uncorrelated pairs [36], is however still very model dependent, and no unambiguous experimental signal for it has been found yet. Possible ways of constraining this contribution will be discussed in this section.

Experimentally, the higher mass of bottomonia compared to charmonia implies higher p_{T} decay leptons, allowing the ATLAS and CMS experiments to measure the production down to zero transverse momentum, as is possible for ALICE for both charmonia and bottomonia [72, 73]. The proximity in mass between the different mass states, especially between the $\Upsilon(2\mathrm{S})$ and $\Upsilon(3\mathrm{S})$ states, also means that good muon (or electron) momentum resolution is essential to their measurement, especially for excited states.

It is useful to remind quickly the status in 2018, based on results from Run 1 and early Run 2 LHC data as well as RHIC data. Υ production is found to be suppressed in Pb–Pb compared to expectations from a scaling of incoherent pp collisions, in all rapidity, p_{T} and centrality ranges measured [72–75]. Suppression is stronger in central events, as expected from the hotter and longer-lived medium in such events. The results from the most central collisions suggest that a certain amount of suppression of the directly produced $\Upsilon(1\mathrm{S})$ might be needed to explain the data in addition to cold nuclear matter effects and melting of the excited Υ and χ_{b} states. The excited states $\Upsilon(2\mathrm{S})$ and $\Upsilon(3\mathrm{S})$ show higher suppression wrt the ground state, with R_{AA} values which respect the hierarchy expected based on their binding energies. The $\Upsilon(3\mathrm{S})$ is still unobserved in Pb–Pb collisions ($R_{\mathrm{AA}}(\Upsilon(3\mathrm{S})) < 0.094$ at 95% confidence level, for

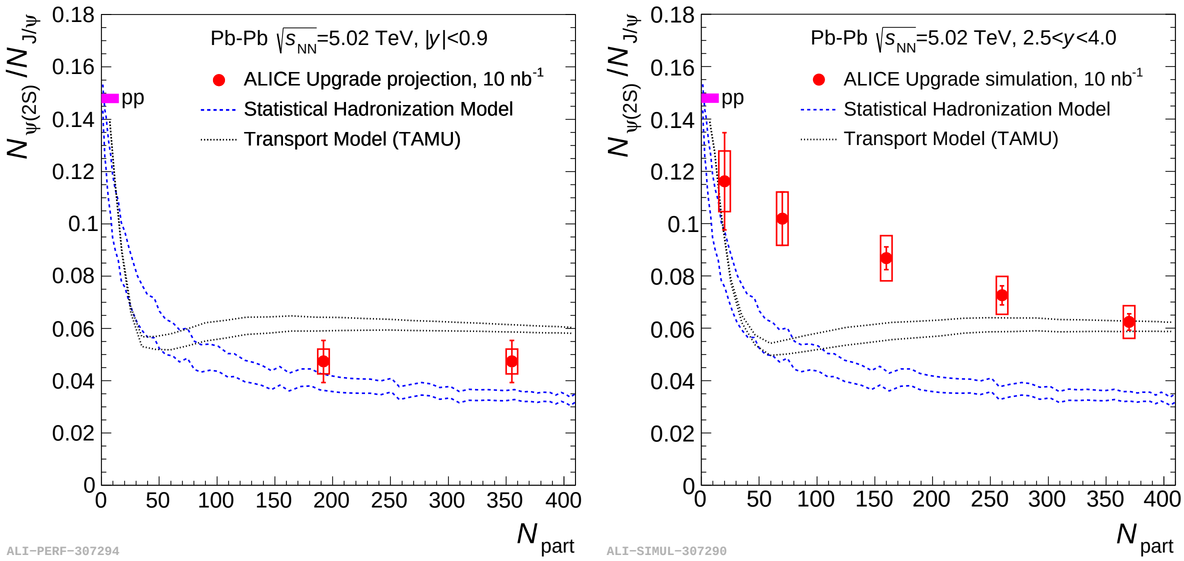

Fig. 4: Production ratio ψ(2S)/J/ψ vs. N_{part} for $|y| < 0.9$ (left) and $2.5 < y < 4$ (right) [63, 68]. Model predictions in the transport approach [62] and from statistical hadronisation [18] are included. The values of the ratio used for the projections are quasi-arbitrary.

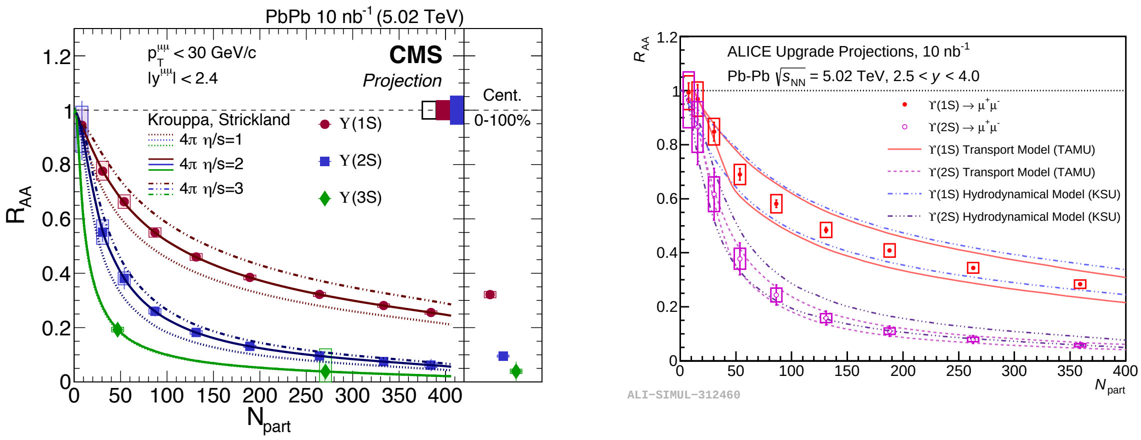

Fig. 5: Centrality dependence of Υ(1S), Υ(2S) and Υ(3S) R_{AA}, as projected by the CMS [69, 77] (left) and ALICE (centre) experiments, and from a transport model [19]

$\sqrt{s_{NN}} = 5.02$ TeV [74, 76]). No significant dependence of the suppression of Υ states is found at the LHC on collision energy or rapidity.

Differences exist between models in the theoretical treatment of the suppression of the bottomonia in the medium, as summarised earlier in Section. 1.1. Different assumptions are used regarding the production mechanism, the heavy quark potential, or the evolution of the quarkonia with the medium. The understanding of hot medium effects will be also improved thanks to higher precision measurements in pp collisions of the feed-down fractions and to stronger constrains of the cold nuclear matter and initial state effects (including nPDF or coherent energy loss effects [78]) from p–Pb collision measurements. Figure 5 shows that the projected uncertainty on the R_{AA} of Υ with 10 nb^{-1} will be much smaller than the current model uncertainties. Bottomonia may bring information complementary to other probes, using the sensitivity of the suppression to the medium shear viscosity or to the initial temperature of the fireball.

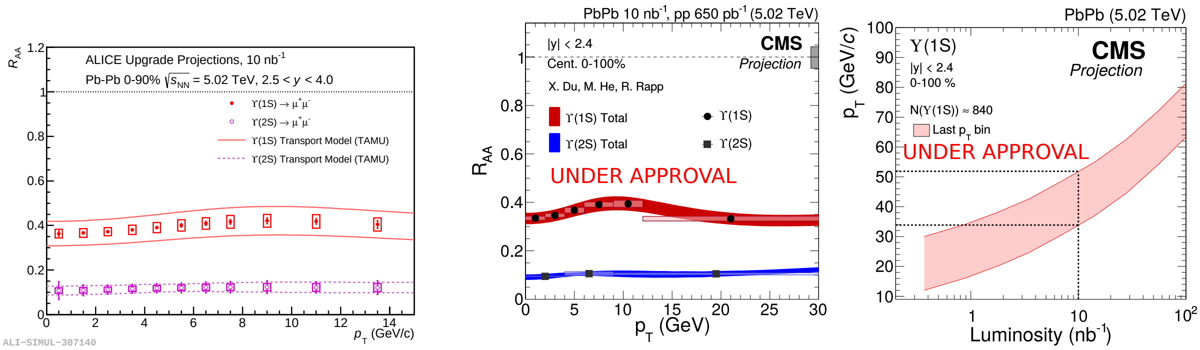

Fig. 6: Projected R_{AA} for $\Upsilon(1S)$ and $\Upsilon(2S)$ expected from the ALICE (left) and CMS [45] (center) experiments, as a function of p_T, with $10\,\mathrm{nb}^{-1}$ of Pb–Pb data. The expected p_T reach for $\Upsilon(1S)$ from the CMS experiment is also shown [45], as the position of the last p_T bin of the measurement, with constant number of observed $\Upsilon(1S)$, as a function of integrated luminosity.

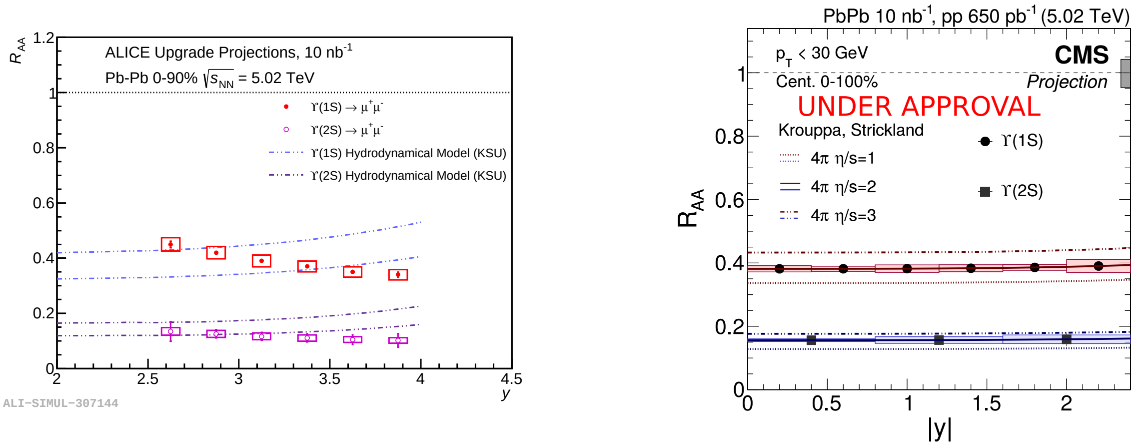

Fig. 7: Projected R_{AA} for $\Upsilon(1S)$ and $\Upsilon(2S)$ expected from the ALICE (left) and CMS [45] (right) experiments, as a function of rapidity, with $10\,\mathrm{nb}^{-1}$ of Pb–Pb data.

A precise measurement of the p_T dependence of the $\Upsilon(1S)$ R_{AA} will be possible using LHC data from Runs 3 & 4. At low and medium p_T, the measurement is sensitive to the possible regeneration component in Υ meson production [19]. Projections for the expected precision of Υ measurements from the ALICE and CMS detectors using an integrated luminosity of $10\,\mathrm{nb}^{-1}$ after the Runs 3 & 4 are shown as a function of p_T in Fig. 6 and y in Fig. 7, and compared to the expectations from two models [19, 20]. In the Kent state model calculations [20] (not shown), where Υ mesons are originating only from the primordial production, with no regeneration component, the R_{AA} is rather flat in the low and medium p_T range. Only at higher p_T (above 10–15 GeV/c) is a small rise predicted, which can be looked for in Runs 3 & 4 data: as can be seen in Fig. 6, it is expected that a measurement up to a p_T of about 50 GeV/c can be performed with the ATLAS and CMS detectors with $10\,\mathrm{nb}^{-1}$ of data. In the TAMU model [19] however, a regeneration component is considered, and several assumptions are explored, especially on the degree of thermalisation of the bottom quarks. It predicts a maximum in the $\Upsilon(1S)$ R_{AA} at a p_T around 10 GeV/c. The current data is not precise enough to confirm or disfavour such a local maximum in the R_{AA}, but Runs 3 & 4 data will allow to conclude.

Almost no rapidity dependence is expected at the LHC for the nuclear modification factor of Υ mesons within the acceptance of ATLAS and CMS ($|\eta| \lesssim 2.5 - 3$), which can be better tested using

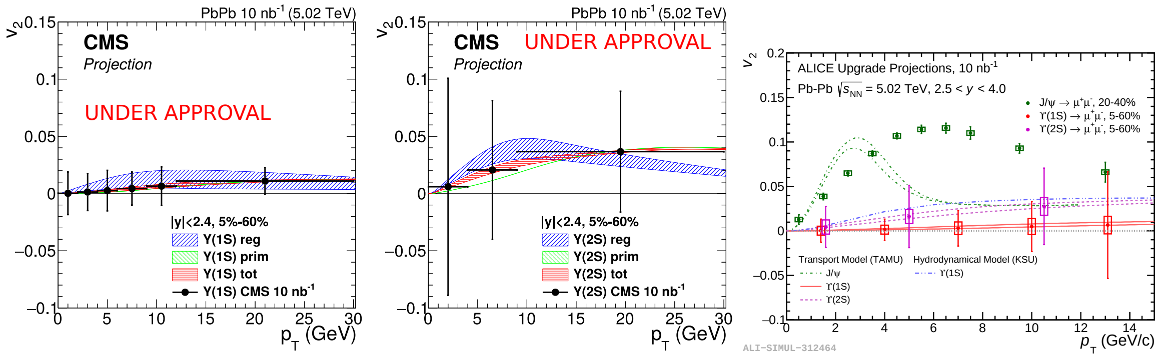

Fig. 8: v_2 projections for the CMS [45] (left and centre) and ALICE (right) experiments for the $\Upsilon(1S)$ and $\Upsilon(2)$ mesons, assuming the predictions from a transport model [19].

Runs 3 & 4 data. This will be further made significant considering the ALICE acceptance ($2.5 < y < 4$), allowing to confirm or disprove the prediction of the hydrodynamic model, see Fig. 7.

Coming back to the matter of regeneration, much can be learnt about it by a measurement of the elliptic flow of $\Upsilon(1S)$ mesons [79], unmeasured to date in any collision system. A parallel can be drawn with that of J/ψ, which is still not properly described by models. This observable requires a more detailed implementation of the dynamics of the interactions between the quarkonium and the medium: thermalisation of the heavy quarks, time dependence of regeneration, path length dependence of energy loss, as well as initial geometry fluctuations and elastic rescattering of the quarkonia in the medium. Thus, collective flow brings complementary information to the R_{AA}, and its measurement can help disentangle some effects. In the case of $\Upsilon(1S)$ mesons, a small v_2 (order of 1–2%) is expected [19, 80, 81], as can be seen in Fig. 8.The elliptic flow of $\Upsilon(2S)$ could be significantly higher [19, 81], both from the regenerated and primordial components. For both states, projections show that experimental precision may not be enough for a significant v_2 measurement, assuming v_2 values as in Ref. [19]. For this reason, combining results between the different LHC experiments would be beneficial to reach a better sensitivity.

While we have focused on the R_{AA} and v_2 in this section, bottomonium production can be studied using other observables. For instance, fully corrected yields or cross sections in Pb–Pb can be studied, without making the ratio to a pp measurement in a R_{AA}. Such a measurement, already reported in some of the available experimental results [74], can directly be compared to production models.

1.4 Quarkonia in p–Pb and pp collisions

1.4.1 p–Pb *collisions*

Quarkonium-production studies in high-energy p–Pb collisions are usually carried out to measure how much specific nuclear effects, those which do *not* result from the creation of a deconfined state of matter, can alter the quarkonium yields. They should indeed be accounted for in the interpretation of Pb–Pb results. They are also interesting on their own as they provide means to probe the modification of the gluon densities in the nuclei, the interaction between such pure heavy-quark bound states and light hadrons, or phenomena such as the coherent medium-induced energy loss of these quark-antiquark pairs. The measurements as a function of event activity brought several surprises, hotly discussed presently.

Usually, a separation into initial-state and final-state effects is done (coherent energy loss effects [82] can be seen as an interplay between the two types of effects). Yet, it is probably more instructive to separate out the effects which are believed to impact *all* the states of the charmonium or the bottomonium family with the *same* magnitude from those which are expected to impact differently the ground and the excited states. In principle, initial-state effects (in particular gluon shadowing [83]) are of the first kind as the nature of the to-be-produced quarkonium state is not yet fixed when the effects are at work. On the contrary, final-state effects (like regeneration [84]) do depend on the properties of the produced quarkonium state and are thus be of the second kind.

However, in p–Pb collisions at LHC energies, final-state interactions between the heavy-quark pair and the nuclear matter likely occur *before* the pair hadronises. This is due to the large boost between the nucleus and the pair – and thus the quarkonium. At rest, a $c\bar{c}$ or $b\bar{b}$ pair takes 0.3–0.4 fm/c to hadronise; seen from the nucleus, at, for instance $y^{\rm lab}_{\rm pair} - y_{\rm beam} \sim 7$, it takes $\gamma = \cosh(7) \simeq 500$ times longer. As such, final-state interactions with the compounds nucleus likely do not discriminate ground and excited quarkonium states, unless rescattering in the nucleus affects the $\mathrm{Q\bar{Q}}$ wave function, overlapping with the quarkonium wave function at large distance [85]. Such an argument based on the existence of a large boost is nevertheless not applicable if one considers effects arising from the interactions between the pair and other particles *produced* by the p–Pb collisions, not those contained in the Pb nucleus. The former are indeed not moving at the Pb projectile rapidity. In fact, some of these particles can have similar rapidities as the quarkonium and can thus be considered as comoving with it [86–88].

The simultaneous study of open-heavy flavoured hadrons along with both ground and excited quarkonium states can shed light on all these phenomena. Along the lines exposed above, one expects forward-quarkonium production in p–Pb collisions (namely when the quarkonia flies in the direction of the proton) to be sensitive to low-x phenomena (like the gluon shadowing or saturation in the lead ion) and to the coherent energy loss. On the contrary, the backward production should be sensitive to the gluon antishadowing and to fully coherent energy loss. Moreover, the scatterings of quarkonia with comoving particles occur more often backward than forward, due to the rapidity-asymmetric particle multiplicities, and more often as well with the larger and less tightly bound excited states.

With a wide rapidity coverage spanning from about -5 to 5, the LHC data from the 4 experiments are unique as they allow one to probe much smaller x values than at RHIC and with a larger reach in $p_{\rm T}$. The higher c.m.s. energy, the competitive luminosities and the resolution of the detectors also allow for more extensive studies of the bottomonium family. In fact, an important observation made with Run 1 data was that of a relative suppression in p–Pb collisions of the excited $\Upsilon(2S)$,$\Upsilon(3S)$ states compared to that of the $\Upsilon(1S)$ observed by CMS [89] as a function of the event activity (recently confirmed by ATLAS [90], but also observed in pp collisions by CMS [91]). Not only was it unexpected, but it constitutes a challenge to the conventional interpretation of suppression observed in Pb–Pb collisions [74, 76, 92], which is of a significantly larger magnitude, but of a similar pattern. Such a relative suppression was also observed in the charmonium sector [93], where it is as well remarkable.

As far as the suppression of the $\Upsilon(1S)$ and J/ψ is concerned, they seem to follow the expectations based on the RHIC results with a strong forward suppression described by shadowing – of a compatible magnitude to that observed with HF data [83], or with the coherent energy loss mechanism [82]. More data, including that on $\Upsilon(nS)$ and Drell-Yan production, are clearly needed to disentangle both effects [94] (see also Section **??**). More precision for $\Upsilon(nS)$ and non-prompt J/ψ is in general critically needed as the typical experimental uncertainties are still on the order of the expected effects. As a case in point, backward y data are not yet precise enough to quantify the magnitude of the gluon antishadowing, see Section **??** for the possible relevance of quarkonium p–Pb LHC data on nuclear PDF fits. Direct inclusion of this data in nPDF fits is however not yet possible, pending unambiguous clarification of the different effects impacting quarkonium production in p–Pb collisions.

Recently, the measurement of v_2 of J/ψ in p–Pb collisions became available [95, 96], indicating a large azimuthal anisotropy, $v_2 \lesssim 0.1$ up to $p_{\rm T} \lesssim 8$ GeV/c. Recent transport model calculations [84], which are successful in describing the features of the data, including the transverse momentum and centrality dependence of J/ψ and $\psi(2S)$ production in p–Pb, cannot reach the high value of the v_2 coefficient seen in data [95, 96] (see Fig. 9), suggesting that the observed v_2 in p–Pb collisions might also originate from initial state effects. A precision measurement in Runs 3 & 4 for a broad rapidity range will clarify this.

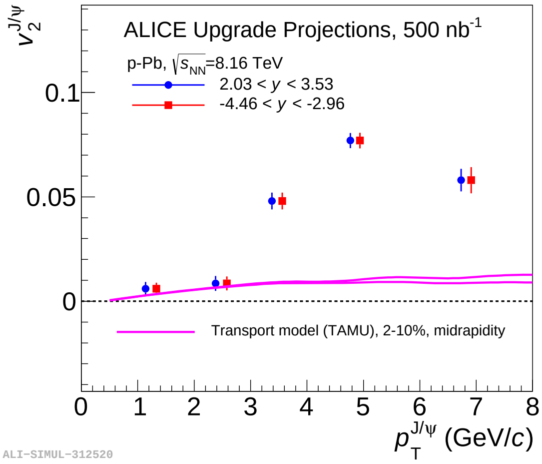

Fig. 9: The p_{T} dependence of the v_2 coefficient of J/ψ mesons in p–Pb collisions, for 500 nb^{-1} (ALICE). The projections are based on current ALICE data for 0–20% centrality [95] and are shown separately for negative and positive y_{CM}), assuming the same magnitude and are compared with transport model (TAMU) calculations [84] for midrapidity.

In addition to conventional LHC collider data, one should not overlook the discriminating power of data which can be collected in the fixed-target mode [97, 98]. Not only they correspond to completely different energy and (c.m.s.) rapidity ranges, but extremely competitive luminosities, up to a few fb^{-1}, are easily reachable, beyond what can be reached in the collider mode during Runs 3 & 4. The LHCb collaboration has paved the way for a full fixed-target program at the LHC with their SMOG luminosity monitor [99] used as an internal (He, Ne, Ar) gas target [100] (see also Section **??**). It is now clear that corresponding studies to those suggested above are possible [101] with the LHCb and ALICE detectors with minor technical adjustments. They would drastically expand the scope of current proton-nucleus quarkonium studies.

1.4.2 High-multiplicity pp *collisions*

Systematic studies of the quarkonium production in high-multiplicity pp events can play an important role in understanding hadronisation. In particular, the correlation of the quarkonium yields with the charged-particle multiplicity can provide new insights into the interplay between hard and soft processes in particle production. Hidden and open heavy-flavour production measurements as a function of the event activity were carried out at the LHC during Run 1 [89, 102]. The striking feature of the data is that the production yields of quarkonia in high multiplicity events are significantly enhanced relative to minimum bias events, like for D mesons [103]. Specifically, the measurements of the self-normalised yields (the yield divided by the mean yield in minimum bias collisions) as a function of the self-normalised charged-particle multiplicity show an increase which is stronger than linear at the highest multiplicities. The similarity between the D-meson and J/ψ results [102, 103] suggests that this behaviour is most likely related to the production processes, and that hadronisation may only play a secondary role. When comparing J/ψ preliminary results at $\sqrt{s} = 13$ TeV [104] to the ones previously obtained at $\sqrt{s} = 7$ TeV [102], no significant energy dependence is observed, *i.e.* the relative J/ψ yields for events with identical relative multiplicities give similar results. In addition, a dependence of the excited-to-ground-state ratio with charged particle multiplicity is observed in the bottomonium sector in pp collisions [89, 91].

The data are described both by initial-state models as well as by a model assuming hydrodynamic evolution [105], considering that the energy density reached in pp collisions at LHC is high enough to apply such evolution. Initial-state (saturation) effects are considered within i) the Color-Glass-Condensate (CGC) framework [106]; ii) the percolation approach [107, 108]; iii) a model with higher Fock states [109], based on parameters derived from $\mathrm{p–Pb}$ collisions. The energy dependence of the cross sections is controlled by the saturation momentum $Q_s(x)$ in the case of the CGC or density of colour ropes $\rho_s(y, p_T)$ in the percolation model, which also governs the charged-hadron multiplicity; events at different energies with the same Q_s or ρ_s are therefore identical. For a given event multiplicity, they predict the relative yields to be almost energy independent. It seems that, in any case, multiple interactions at the partonic level need to be taken into account in order to reproduce the data [110–112].

Runs 3 & 4 data, reaching unprecedented high multiplicities because of larger data samples, and allowing for differential studies in p_{T}, will certainly help discriminate models. For instance, in the percolation model, where colour interactions produce a reduction of the charged-particle multiplicities, the deviation from the linear behaviour is expected to be steeper for high-p_{T} quarkonia (and D mesons). Moreover, measurements of J/ψ yields relative to those of D mesons with the same transverse mass could help elucidate the relative contribution of hadronisation and initial-state effects.

Studies of double differential ratios of excited-to-ground quarkonium states versus relative multiplicity could help clarify the presence of final-state effects, either QGP-like or the ones proposed by the comover model [113, 114]. Also, within the CGC+NRQCD framework [106], the relative contributions of the 4 leading J/ψ Fock states have been calculated as a function of the event activity, showing a different dependence for different Fock states.

References

[1] E. Eichten, K. Gottfried, T. Kinoshita, K. D. Lane, and T.-M. Yan, *Charmonium: Comparison with Experiment*, Phys. Rev. **D21** (1980) 203.

[2] G. S. Bali, *QCD forces and heavy quark bound states*, Phys. Rept. **343** (2001) 1–136, `arXiv:hep-ph/0001312 [hep-ph]`.

[3] N. Brambilla, A. Pineda, J. Soto, and A. Vairo, *Effective field theories for heavy quarkonium*, Rev. Mod. Phys. **77** (2005) 1423, `arXiv:hep-ph/0410047 [hep-ph]`.

[4] Y. Schroder, *The Static potential in QCD to two loops*, Phys. Lett. **B447** (1999) 321–326, `arXiv:hep-ph/9812205 [hep-ph]`.

[5] N. Brambilla, A. Pineda, J. Soto, and A. Vairo, *Potential NRQCD: An Effective theory for heavy quarkonium*, Nucl. Phys. **B566** (2000) 275, `arXiv:hep-ph/9907240 [hep-ph]`.

[6] Quarkonium Working Group Collaboration, N. Brambilla et al., *Heavy quarkonium physics*, `arXiv:hep-ph/0412158 [hep-ph]`.

[7] R. Rapp, D. Blaschke, and P. Crochet, *Charmonium and bottomonium production in heavy-ion collisions*, Prog. Part. Nucl. Phys. **65** (2010) 209–266, `arXiv:0807.2470 [hep-ph]`.

[8] P. Braun-Munzinger and J. Stachel, *Charmonium from Statistical Hadronization of Heavy Quarks: A Probe for Deconfinement in the Quark-Gluon Plasma*, Landolt-Bornstein **23** (2010) 424, `arXiv:0901.2500 [nucl-th]`.

[9] L. Kluberg and H. Satz, *Color Deconfinement and Charmonium Production in Nuclear Collisions*, `arXiv:0901.3831 [hep-ph]`.

[10] A. Mocsy, P. Petreczky, and M. Strickland, *Quarkonia in the Quark Gluon Plasma*, Int. J. Mod. Phys. **A28** (2013) 1340012, `arXiv:1302.2180 [hep-ph]`.

[11] Y. Liu, K. Zhou, and P. Zhuang, *Quarkonia in high energy nuclear collisions*, Int. J. Mod. Phys. **E24** (2015) no. 11, 1530015.

[12] S. Y. F. Liu and R. Rapp, *Spectral and Transport Properties of a Non-Perturbative Quark-Gluon Plasma*, `arXiv:1612.09138 [nucl-th]`.

[13] T. Matsui and H. Satz, *J/ψ Suppression by Quark-Gluon Plasma Formation*, Phys. Lett. **B178** (1986) 416–422.

[14] P. Braun-Munzinger and J. Stachel, *(Non)thermal aspects of charmonium production and a new look at J / psi suppression*, Phys. Lett. **B490** (2000) 196–202, `arXiv:nucl-th/0007059 [nucl-th]`.

[15] R. L. Thews, M. Schroedter, and J. Rafelski, *Enhanced J/ψ production in deconfined quark matter*, Phys. Rev. **C63** (2001) 054905, `arXiv:hep-ph/0007323 [hep-ph]`.

[16] C. Young and E. Shuryak, *Charmonium in strongly coupled quark-gluon plasma*, Phys. Rev. **C79** (2009) 034907, `arXiv:0803.2866 [nucl-th]`.

[17] R. Rapp and X. Du, *Theoretical Perspective on Quarkonia from SPS via RHIC to LHC*, Nucl. Phys. **A967** (2017) 216–224, `arXiv:1704.07923 [hep-ph]`.

[18] A. Andronic, P. Braun-Munzinger, K. Redlich, and J. Stachel, *Decoding the phase structure of QCD via particle production at high energy*, Nature **561** (2018) 321–330, `arXiv:1710.09425 [nucl-th]`.

[19] X. Du, R. Rapp, and M. He, *Color Screening and Regeneration of Bottomonia in High-Energy Heavy-Ion Collisions*, Phys. Rev. **C96** (2017) no. 5, 054901, `arXiv:1706.08670 [hep-ph]`.

[20] B. Krouppa, A. Rothkopf, and M. Strickland, *Bottomonium suppression using a lattice QCD vetted potential*, Phys. Rev. **D97** (2018) no. 1, 016017, `arXiv:1710.02319 [hep-ph]`.

[21] C.-Y. Wong, *Heavy quarkonia in quark-gluon plasma*, Phys. Rev. **C72** (2005) 034906, `arXiv:hep-ph/0408020 [hep-ph]`.

[22] A. Mocsy and P. Petreczky, *Quarkonia correlators above deconfinement*, Phys. Rev. **D73** (2006)

074007, arXiv:hep-ph/0512156 [hep-ph].

[23] W. M. Alberico, A. Beraudo, A. De Pace, and A. Molinari, *Quarkonia in the deconfined phase: Effective potentials and lattice correlators*, Phys. Rev. **D75** (2007) 074009, arXiv:hep-ph/0612062 [hep-ph].

[24] N. Brambilla, J. Ghiglieri, A. Vairo, and P. Petreczky, *Static quark-antiquark pairs at finite temperature*, Phys. Rev. **D78** (2008) 014017, arXiv:0804.0993 [hep-ph].

[25] F. Riek and R. Rapp, *Selfconsistent Evaluation of Charm and Charmonium in the Quark-Gluon Plasma*, New J. Phys. **13** (2011) 045007, arXiv:1012.0019 [nucl-th].

[26] Y. Burnier, O. Kaczmarek, and A. Rothkopf, *Quarkonium at finite temperature: Towards realistic phenomenology from first principles*, JHEP **12** (2015) 101, arXiv:1509.07366 [hep-ph].

[27] S. Y. F. Liu and R. Rapp, *T-matrix Approach to Quark-Gluon Plasma*, Phys. Rev. **C97** (2018) no. 3, 034918, arXiv:1711.03282 [nucl-th].

[28] G. Bhanot and M. E. Peskin, *Short Distance Analysis for Heavy Quark Systems. 2. Applications*, Nucl. Phys. **B156** (1979) 391–416.

[29] D. Kharzeev and H. Satz, *Quarkonium interactions in hadronic matter*, Phys. Lett. **B334** (1994) 155–162, arXiv:hep-ph/9405414 [hep-ph].

[30] L. Grandchamp and R. Rapp, *Thermal versus direct J/ψ production in ultrarelativistic heavy ion collisions*, Phys. Lett. **B523** (2001) 60–66, arXiv:hep-ph/0103124 [hep-ph].

[31] M. Laine, O. Philipsen, P. Romatschke, and M. Tassler, *Real-time static potential in hot QCD*, JHEP **03** (2007) 054, arXiv:hep-ph/0611300 [hep-ph].

[32] Y. Park, K.-I. Kim, T. Song, S. H. Lee, and C.-Y. Wong, *Widths of quarkonia in quark gluon plasma*, Phys. Rev. **C76** (2007) 044907, arXiv:0704.3770 [hep-ph].

[33] J.-P. Blaizot, D. De Boni, P. Faccioli, and G. Garberoglio, *Heavy quark bound states in a quark-gluon plasma: Dissociation and recombination*, Nucl. Phys. **A946** (2016) 49–88, arXiv:1503.03857 [nucl-th].

[34] R. Katz and P. B. Gossiaux, *The Schrödinger-Langevin equation with and without thermal fluctuations*, Annals Phys. **368** (2016) 267–295, arXiv:1504.08087 [quant-ph].

[35] S. Kajimoto, Y. Akamatsu, M. Asakawa, and A. Rothkopf, *Dynamical dissociation of quarkonia by wave function decoherence*, Phys. Rev. **D97** (2018) no. 1, 014003, arXiv:1705.03365 [nucl-th].

[36] P. Petreczky and C. Young, *Sequential bottomonium production at high temperatures*, Few Body Syst. **58** (2017) no. 2, 61, arXiv:1606.08421 [nucl-th].

[37] Y. Akamatsu, *Heavy quark master equations in the Lindblad form at high temperatures*, Phys. Rev. **D91** (2015) no. 5, 056002, arXiv:1403.5783 [hep-ph].

[38] N. Brambilla, M. A. Escobedo, J. Soto, and A. Vairo, *Quarkonium suppression in heavy-ion collisions: an open quantum system approach*, Phys. Rev. **D96** (2017) no. 3, 034021, arXiv:1612.07248 [hep-ph].

[39] T. Song, C. M. Ko, and S. H. Lee, *Quarkonium formation time in relativistic heavy-ion collisions*, Phys. Rev. **C91** (2015) no. 4, 044909, arXiv:1502.05734 [nucl-th].

[40] J. Hoelck, F. Nendzig, and G. Wolschin, *In-medium Υ suppression and feed-down in UU and PbPb collisions*, Phys. Rev. **C95** (2017) no. 2, 024905, arXiv:1602.00019 [hep-ph].

[41] S. Aronson, E. Borras, B. Odegard, R. Sharma, and I. Vitev, *Collisional and thermal dissociation of J/ψ and Υ states at the LHC*, Phys. Lett. **B778** (2018) 384–391, arXiv:1709.02372 [hep-ph].

[42] X. Yao and B. Müller, *Approach to equilibrium of quarkonium in quark-gluon plasma*, Phys. Rev. **C97** (2018) no. 1, 014908, arXiv:1709.03529 [hep-ph]. [Erratum: Phys. Rev.C97,no.4,049903(2018)].

[43] A. Beraudo et al., *Extraction of Heavy-Flavor Transport Coefficients in QCD Matter*, arXiv:1803.03824 [nucl-th].

[44] D. Contardo, M. Klute, J. Mans, L. Silvestris, and J. Butler, *Technical Proposal for the Phase-II Upgrade of the CMS Detector*, .

[45] CMS Collaboration, *Projected Heavy Ion Physics Performance at the High Luminosity LHC Era: heavy flavour and quarkonia*, CMS-PAS-FTR-18-024, CERN, Geneva, 2018. https://cds.cern.ch/record/xxxxxx.

[46] ALICE Collaboration, B. Abelev et al., *J/ψ suppression at forward rapidity in Pb-Pb collisions at $\sqrt{s_{NN}} = 2.76$ TeV*, Phys. Rev. Lett. **109** (2012) 072301, arXiv:1202.1383 [hep-ex].

[47] ALICE Collaboration, B. B. Abelev et al., *Centrality, rapidity and transverse momentum dependence of J/ψ suppression in Pb-Pb collisions at $\sqrt{s_{\rm NN}}$=2.76 TeV*, Phys. Lett. **B734** (2014) 314–327, arXiv:1311.0214 [nucl-ex].

[48] ALICE Collaboration, J. Adam et al., *J/ψ suppression at forward rapidity in Pb-Pb collisions at $\sqrt{\rm s_{NN}} = \mathbf{5.02}$ TeV*, Phys. Lett. **B766** (2017) 212–224, arXiv:1606.08197 [nucl-ex].

[49] X. Zhao and R. Rapp, *Medium Modifications and Production of Charmonia at LHC*, Nucl. Phys. **A859** (2011) 114–125, arXiv:1102.2194 [hep-ph].

[50] L. Yan, P. Zhuang, and N. Xu, *Competition between J / psi suppression and regeneration in quark-gluon plasma*, Phys. Rev. Lett. **97** (2006) 232301, arXiv:nucl-th/0608010 [nucl-th].

[51] CMS Collaboration, A. M. Sirunyan et al., *Measurement of prompt and nonprompt charmonium suppression in PbPb collisions at 5.02 TeV*, Eur. Phys. J. **C78** (2018) no. 6, 509, arXiv:1712.08959 [nucl-ex].

[52] ALICE Collaboration, B. B. Abelev et al., *Azimuthal anisotropy of D meson production in Pb-Pb collisions at $\sqrt{s_{\rm NN}} = 2.76$ TeV*, Phys. Rev. **C90** (2014) no. 3, 034904, arXiv:1405.2001 [nucl-ex].

[53] ALICE Collaboration, S. Acharya et al., *D-meson azimuthal anisotropy in midcentral Pb-Pb collisions at $\sqrt{\rm s_{NN}} = \mathbf{5.02}$ TeV*, Phys. Rev. Lett. **120** (2018) no. 10, 102301, arXiv:1707.01005 [nucl-ex].

[54] CMS Collaboration, A. M. Sirunyan et al., *Measurement of prompt D^0 meson azimuthal anisotropy in Pb-Pb collisions at $\sqrt{s_{NN}}$ = 5.02 TeV*, Phys. Rev. Lett. **120** (2018) no. 20, 202301, arXiv:1708.03497 [nucl-ex].

[55] CMS Collaboration, V. Khachatryan et al., *Suppression and azimuthal anisotropy of prompt and nonprompt J/ψ production in PbPb collisions at $\sqrt{s_{\rm NN}} = 2.76$ TeV*, Eur. Phys. J. **C77** (2017) no. 4, 252, arXiv:1610.00613 [nucl-ex].

[56] ALICE Collaboration, E. Abbas et al., *J/Psi Elliptic Flow in Pb-Pb Collisions at $\sqrt{s_{\rm NN}}$ = 2.76 TeV*, Phys. Rev. Lett. **111** (2013) 162301, arXiv:1303.5880 [nucl-ex].

[57] ALICE Collaboration, S. Acharya et al., *J/ψ elliptic flow in Pb-Pb collisions at $\sqrt{s_{\rm NN}} = 5.02$ TeV*, Phys. Rev. Lett. **119** (2017) no. 24, 242301, arXiv:1709.05260 [nucl-ex].

[58] ATLAS Collaboration, M. Aaboud et al., *Prompt and non-prompt J/ψ elliptic flow in Pb+Pb collisions at $\sqrt{s_{_{NN}}} = 5.02$ Tev with the ATLAS detector*, Eur. Phys. J. **C78** (2018) no. 9, 784, arXiv:1807.05198 [nucl-ex].

[59] ALICE Collaboration, S. Acharya et al., *Study of J/ψ azimuthal anisotropy at forward rapidity in Pb-Pb collisions at $\sqrt{s_{\rm NN}}$ = 5.02 TeV*, arXiv:1811.12727 [nucl-ex].

[60] ALICE Collaboration, S. Acharya et al., *Event-shape engineering for the D-meson elliptic flow in mid-central Pb-Pb collisions at $\sqrt{s_{\rm NN}} = 5.02$ TeV*, arXiv:1809.09371 [nucl-ex].

[61] K. Zhou, N. Xu, Z. Xu, and P. Zhuang, *Medium effects on charmonium production at ultrarelativistic energies available at the CERN Large Hadron Collider*, Phys. Rev. **C89** (2014)

no. 5, 054911, `arXiv:1401.5845 [nucl-th]`.

[62] X. Du and R. Rapp, *Sequential Regeneration of Charmonia in Heavy-Ion Collisions*, Nucl. Phys. **A943** (2015) 147–158, `arXiv:1504.00670 [hep-ph]`.

[63] ALICE Collaboration, B. Abelev et al., *Upgrade of the ALICE Experiment: Letter Of Intent*, J. Phys. **G41** (2014) 087001.

[64] ATLAS Collaboration, M. Aaboud et al., *Prompt and non-prompt J/ψ and $\psi(2\mathrm{S})$ suppression at high transverse momentum in 5.02 TeV Pb+Pb collisions with the ATLAS experiment*, Eur. Phys. J. **C78** (2018) no. 9, 762, `arXiv:1805.04077 [nucl-ex]`.

[65] B. Z. Kopeliovich, I. K. Potashnikova, I. Schmidt, and M. Siddikov, *Survival of charmonia in a hot environment*, Phys. Rev. **C91** (2015) no. 2, 024911, `arXiv:1409.5147 [hep-ph]`.

[66] M. Spousta, *On similarity of jet quenching and charmonia suppression*, Phys. Lett. **B767** (2017) 10–15, `arXiv:1606.00903 [hep-ph]`.

[67] F. Arleo, *Quenching of Hadron Spectra in Heavy Ion Collisions at the LHC*, Phys. Rev. Lett. **119** (2017) no. 6, 062302, `arXiv:1703.10852 [hep-ph]`.

[68] ALICE Collaboration, *Addendum of the Letter of Intent for the upgrade of the ALICE experiment : The Muon Forward Tracker*, CERN-LHCC-2013-014. LHCC-I-022-ADD-1, CERN, Geneva, Aug, 2013. `https://cds.cern.ch/record/1592659`.

[69] CMS Collaboration, *Projected Heavy Ion Physics Performance at the High Luminosity LHC Era with the CMS Detector*, CMS-PAS-FTR-17-002, CERN, Geneva, 2017. `https://cds.cern.ch/record/2291105`.

[70] A. Andronic et al., *Heavy-flavour and quarkonium production in the LHC era: from proton–proton to heavy-ion collisions*, Eur. Phys. J. **C76** (2016) no. 3, 107, `arXiv:1506.03981 [nucl-ex]`.

[71] LHCb Collaboration, R. Aaij et al., *Study of χ_{b} meson production in $\mathrm{p}\,\mathrm{p}$ collisions at $\sqrt{s} = 7$ and $8\,\mathrm{TeV}$ and observation of the decay $\chi_{\mathrm{b}}(3\mathrm{P}) \to \Upsilon(3\mathrm{S})\gamma$*, Eur. Phys. J. **C74** (2014) no. 10, 3092, `arXiv:1407.7734 [hep-ex]`.

[72] ALICE Collaboration, B. B. Abelev et al., *Suppression of $\Upsilon(1S)$ at forward rapidity in Pb-Pb collisions at $\sqrt{s_{\mathrm{NN}}} = 2.76$ TeV*, Phys. Lett. **B738** (2014) 361–372, `arXiv:1405.4493 [nucl-ex]`.

[73] ALICE Collaboration, S. Acharya et al., *Υ suppression at forward rapidity in Pb-Pb collisions at $\sqrt{s_{\mathrm{NN}}}$ = 5.02 TeV*, `arXiv:1805.04387 [nucl-ex]`.

[74] CMS Collaboration, A. M. Sirunyan et al., *Measurement of nuclear modification factors of Υ(1S), Υ(2S), and Υ(3S) mesons in PbPb collisions at $\sqrt{s_{_{\mathrm{NN}}}} = 5.02$ TeV*, `arXiv:1805.09215 [hep-ex]`.

[75] CMS Collaboration, V. Khachatryan et al., *Suppression of $\Upsilon(1S)$, $\Upsilon(2S)$ and $\Upsilon(3S)$ production in PbPb collisions at $\sqrt{s_{\mathrm{NN}}}$ = 2.76 TeV*, Phys. Lett. **B770** (2017) 357–379, `arXiv:1611.01510 [nucl-ex]`.

[76] CMS Collaboration, A. M. Sirunyan et al., *Suppression of Excited Υ States Relative to the Ground State in Pb-Pb Collisions at $\sqrt{s_{\mathrm{NN}}}$=5.02 TeV*, Phys. Rev. Lett. **120** (2018) no. 14, 142301, `arXiv:1706.05984 [hep-ex]`.

[77] B. Krouppa and M. Strickland, *Predictions for bottomonia suppression in 5.023 TeV Pb-Pb collisions*, Universe **2** (2016) no. 3, 16, `arXiv:1605.03561 [hep-ph]`.

[78] F. Arleo and S. Peigné, *Quarkonium suppression in heavy-ion collisions from coherent energy loss in cold nuclear matter*, JHEP **10** (2014) 73, `arXiv:1407.5054 [hep-ph]`.

[79] D. Das and N. Dutta, *Anisotropic flow: A case for Bottomonia*, Int. J. Mod. Phys. **A33** (2018) no. 16, 1850092, `arXiv:1802.00414 [nucl-ex]`.

[80] X. Yao, W. Ke, Y. Xu, S. Bass, and B. Müller, *Quarkonium production in heavy ion collisions:*

coupled Boltzmann transport equations, in *27th International Conference on Ultrarelativistic Nucleus-Nucleus Collisions (Quark Matter 2018) Venice, Italy, May 14-19, 2018*. 2018. arXiv:1807.06199 [nucl-th].

[81] P. P. Bhaduri, N. Borghini, A. Jaiswal, and M. Strickland, *Anisotropic escape mechanism and elliptic flow of bottomonia*, arXiv:1809.06235 [hep-ph].

[82] F. Arleo, S. Peigné, and T. Sami, *Revisiting scaling properties of medium-induced gluon radiation*, Phys. Rev. **D83** (2011) 114036, arXiv:1006.0818 [hep-ph].

[83] A. Kusina, J.-P. Lansberg, I. Schienbein, and H.-S. Shao, *Gluon shadowing in heavy-flavor production at the LHC*, Phys. Rev. Lett. **121** (2018) 052004, arXiv:1712.07024 [hep-ph].

[84] X. Du and R. Rapp, *In-Medium Charmonium Production in Proton-Nucleus Collisions*, arXiv:1808.10014 [nucl-th].

[85] C. J. Benesh, J. Qiu, and J. P. Vary, *J/ψ suppression in hadron-nucleus collisions*, Phys. Rev. C **50** (1994) 1015–1023, arXiv:hep-ph/9403265 [hep-ph].

[86] S. Gavin and R. Vogt, *Charmonium suppression by Comover scattering in Pb + Pb collisions*, Phys. Rev. Lett. **78** (1997) 1006–1009, arXiv:hep-ph/9606460 [hep-ph].

[87] S. J. Brodsky and A. H. Mueller, *USING NUCLEI TO PROBE HADRONIZATION IN QCD*, Phys. Lett. **B206** (1988) 685.

[88] A. Capella, E. G. Ferreiro, and A. B. Kaidalov, *Nonsaturation of the J / psi suppression at large transverse energy in the comovers approach*, Phys. Rev. Lett. **85** (2000) 2080–2083, arXiv:hep-ph/0002300 [hep-ph].

[89] CMS Collaboration, S. Chatrchyan et al., *Event activity dependence of Y(nS) production in $\sqrt{s_{NN}}$=5.02 TeV pPb and $\sqrt{s}$=2.76 TeV pp collisions*, JHEP **04** (2014) 103, arXiv:1312.6300 [nucl-ex].

[90] ATLAS Collaboration, M. Aaboud et al., *Measurement of quarkonium production in proton-lead and proton-proton collisions at* 5.02 TeV *with the ATLAS detector*, Eur. Phys. J. **C78** (2018) no. 3, 171, arXiv:1709.03089 [nucl-ex].

[91] CMS Collaboration, *Dependence of the Υ(nS) production ratios on charged particle multiplicity in pp collisions at $\sqrt{s} = 7$ TeV*, CMS-PAS-BPH-14-009, CERN, 2016. https://cds.cern.ch/record/2223879.

[92] CMS Collaboration, S. Chatrchyan et al., *Observation of sequential Upsilon suppression in PbPb collisions*, Phys. Rev. Lett. **109** (2012) 222301, arXiv:1208.2826 [nucl-ex].

[93] ALICE Collaboration, B. B. Abelev et al., *Suppression of ψ(2S) production in pPb collisions at $\sqrt{s_{\mathrm{NN}}} = 5.02$ TeV*, JHEP **12** (2014) 073, arXiv:1405.3796 [nucl-ex].

[94] F. Arleo and S. Peigné, *Disentangling Shadowing from Coherent Energy Loss using the Drell-Yan Process*, Phys. Rev. D **95** (2017) no. 1, 011502, arXiv:1512.01794 [hep-ph].

[95] ALICE Collaboration, S. Acharya et al., *Search for collectivity with azimuthal J/ψ-hadron correlations in high multiplicity p-Pb collisions at $\sqrt{s_{\mathrm{NN}}}$ = 5.02 and 8.16 TeV*, Phys. Lett. **B780** (2018) 7–20, arXiv:1709.06807 [nucl-ex].

[96] CMS Collaboration, A. M. Sirunyan et al., *Observation of prompt J/ψ meson elliptic flow in high-multiplicity pPb collisions at $\sqrt{s_{\mathrm{NN}}} = 8.16$ TeV*, Submitted to: Phys. Lett. (2018) , arXiv:1810.01473 [hep-ex].

[97] S. J. Brodsky, F. Fleuret, C. Hadjidakis, and J. P. Lansberg, *Physics Opportunities of a Fixed-Target Experiment using the LHC Beams*, Phys. Rept. **522** (2013) 239–255, arXiv:1202.6585 [hep-ph].

[98] J. P. Lansberg, S. J. Brodsky, F. Fleuret, and C. Hadjidakis, *Quarkonium Physics at a Fixed-Target Experiment using the LHC Beams*, Few Body Syst. **53** (2012) 11–25, arXiv:1204.5793 [hep-ph].

[99] M. Ferro-Luzzi, *Proposal for an absolute luminosity determination in colliding beam experiments using vertex detection of beam-gas interactions*, Nucl. Instrum. Meth. **A553** (2005) 388–399.

[100] LHCb Collaboration, R. Aaij et al., *First measurement of charm production in fixed-target configuration at the LHC*, `arXiv:1810.07907 [hep-ex]`.

[101] C. Hadjidakis et al., *A Fixed-Target Programme at the LHC: Physics Case and Projected Performances for Heavy-Ion, Hadron, Spin and Astroparticle Studies*, `arXiv:1807.00603 [hep-ex]`.

[102] ALICE Collaboration, B. Abelev et al., *J/ψ Production as a Function of Charged Particle Multiplicity in pp Collisions at $\sqrt{s} = 7$ TeV*, Phys. Lett. **B712** (2012) 165–175, `arXiv:1202.2816 [hep-ex]`.

[103] ALICE Collaboration, J. Adam et al., *Measurement of charm and beauty production at central rapidity versus charged-particle multiplicity in proton-proton collisions at $\sqrt{s} = 7$ TeV*, JHEP **09** (2015) 148, `arXiv:1505.00664 [nucl-ex]`.

[104] ALICE Collaboration, S. G. Weber, *Measurement of J/ψ production as a function of event multiplicity in pp collisions at $\sqrt{s} = 13\,\mathrm{TeV}$ with ALICE*, Nucl. Phys. **A967** (2017) 333–336, `arXiv:1704.04735 [hep-ex]`.

[105] K. Werner, B. Guiot, I. Karpenko, and T. Pierog, *Analysing radial flow features in p-Pb and p-p collisions at several TeV by studying identified particle production in EPOS3*, Phys. Rev. **C89** (2014) no. 6, 064903, `arXiv:1312.1233 [nucl-th]`.

[106] Y.-Q. Ma, P. Tribedy, R. Venugopalan, and K. Watanabe, *Event engineering heavy flavor production and hadronization in high multiplicity hadron-hadron collisions*, `arXiv:1803.11093 [hep-ph]`.

[107] E. G. Ferreiro and C. Pajares, *High multiplicity pp events and J/ψ production at LHC*, Phys. Rev. **C86** (2012) 034903, `arXiv:1203.5936 [hep-ph]`.

[108] E. G. Ferreiro and C. Pajares, *Open charm production in high multiplicity proton-proton events at the LHC*, `arXiv:1501.03381 [hep-ph]`.

[109] B. Z. Kopeliovich, H. J. Pirner, I. K. Potashnikova, K. Reygers, and I. Schmidt, *J/ψ in high-multiplicity pp collisions: Lessons from pA collisions*, Phys. Rev. **D88** (2013) no. 11, 116002, `arXiv:1308.3638 [hep-ph]`.

[110] T. Sjöstrand, S. Ask, J. R. Christiansen, R. Corke, N. Desai, P. Ilten, S. Mrenna, S. Prestel, C. O. Rasmussen, and P. Z. Skands, *An Introduction to PYTHIA 8.2*, Comput. Phys. Commun. **191** (2015) 159–177, `arXiv:1410.3012 [hep-ph]`.

[111] P. Skands, S. Carrazza, and J. Rojo, *Tuning PYTHIA 8.1: the Monash 2013 Tune*, Eur. Phys. J. **C74** (2014) no. 8, 3024, `arXiv:1404.5630 [hep-ph]`.

[112] T. Sjöstrand, *The Development of MPI Modelling in PYTHIA*, `arXiv:1706.02166 [hep-ph]`.

[113] E. G. Ferreiro, *Excited charmonium suppression in proton–nucleus collisions as a consequence of comovers*, Phys. Lett. **B749** (2015) 98–103, `arXiv:1411.0549 [hep-ph]`.

[114] E. G. Ferreiro and J.-P. Lansberg, *Is bottomonium suppression in proton-nucleus and nucleus-nucleus collisions at LHC energies due to the same effects?*, JHEP **10** (2018) 094, `arXiv:1804.04474 [hep-ph]`.